Marine Biotechnology (2019) 21:262–275
https://doi.org/10.1007/s10126-019-09878-x

ORIGINAL ARTICLE

Constructing a High-Density Genetic Linkage Map for Large Yellow Croaker (*Larimichthys crocea*) and Mapping Resistance Trait Against Ciliate Parasite *Cryptocaryon irritans*

Shengnan Kong[1,2,3] · Qiaozhen Ke[1,2] · Lin Chen[2] · Zhixiong Zhou[2] · Fei Pu[1] · Ji Zhao[1] · Huaqiang Bai[2] · Wenzhu Peng[2] · Peng Xu[1,2,4]

Received: 4 December 2018 / Accepted: 18 January 2019 / Published online: 19 February 2019

Abstract

The large yellow croaker (*Larimichthys crocea*) is the most economically important marine cage-farming fish in China in the past decade. However, the sustainable development of large yellow croaker aquaculture has been severely hampered by several diseases, of which, the *white spot* disease caused by ciliate protozoan parasite *Cryptocaryon irritans* ranks the most damaging disease in large yellow croaker cage farms. To better understand the genetic basis of parasite infection and disease resistance to *C. irritans*, it is vital to map the traits and localize the underlying candidate genes in *L. crocea* genome. Here, we constructed a high-density genetic linkage map using double-digest restriction-site associated DNA (ddRAD)-based high-throughput SNP genotyping data of a F1 mapping family, which had been challenged with *C. irritans* for resistant trait measure. A total of 5261 SNPs was grouped and oriented into 24 linkage groups (LGs), representing 24 chromosomes of *L. crocea*. The total genetic map length was 1885.67 cM with an average inter-locus distance of 0.36 cM. Quantitative trait loci (QTL) mapping identified seven significant QTLs in four LGs linked to *C. irritans* disease resistance. Candidate genes underlying disease resistance were identified from the reference genome, including *ifnar1*, *ifngr2*, *ikbke*, and *CD112*. Comparative genomic analysis between large yellow croaker and the four closely related species revealed high evolutionary conservation of chromosomes, though inter-chromosomal rearrangements do exist. Especially, the croaker genome structure was closer to the medaka genome than stickleback, indicating that the croaker genome might retain the teleost ancestral genome structure. The high-density genetic linkage map provides an important tool and resource for fine mapping, comparative genome analysis, and molecular selective breeding of large yellow croaker.

Keywords Large yellow croaker · Genetic linkage map · Comparative genomic · QTL · *Cryptocaryon irritans*

Introduction

The large yellow croaker (*Larimichthys crocea*) is one of the most economically important marine culture fish mainly cultivated in the coastal areas of Southeast China (Jian and Wu 2003). It also represents the largest yield of single fish species of marine net cage aquaculture of China with annual production of approximate 178,000 tons according to the Fishery Annual Statistics 2017 published by the Ministry of Agriculture, China. With the rapid development of aquaculture industry of large yellow croaker, many problems are emerging and hampering the sustainable development of aquaculture, of which, high mortality rate caused by cryptocaryonosis (white spot disease) is one of the most severe disease problems for large yellow croaker aquaculture in the past decade. Cryptocaryonosis is caused by the most

Electronic supplementary material The online version of this article (https://doi.org/10.1007/s10126-019-09878-x) contains supplementary material, which is available to authorized users.

✉ Peng Xu
xupeng77@xmu.edu.cn

[1] State Key Laboratory of Large Yellow Croaker Breeding, Ningde Fufa Fisheries Company Limited, Ningde 352103, China

[2] State Key Laboratory of Marine Environmental Science, College of Ocean and Earth Sciences, Xiamen University, Xiamen 361102, China

[3] College of Fisheries, Henan Normal University, Xinxiang 453007, China

[4] Laboratory for Marine Biology and Biotechnology, Qingdao National Laboratory for Marine Science and Technology, Qingdao 266071, China

common and destructive protozoan pathogen of marine fish, *Cryptocaryon irritans*, which infects fish skin and gills, leading to a devastating effect on cultivated large yellow croaker as well as other cultured marine fishes (Niu et al. 2013; Li et al. 2011). Unfortunately, there are few treatments for eradicating cryptocaryonosis effectively, especially for marine cage farm aquaculture. Selective breeding to improve anti-infection resistance in cultured large yellow croaker becomes promising alternatives for controlling cryptocaryonosis that severely affect croakers. With the rapid development of molecular genetics technology, genetic researches on resistant traits of aquatic animals have also made rapid progresses, such as genetic localization of the lymphocystis disease-resistant traits of Japanese flounder (Fuji et al. 2007), *Ceratomyxa shasta* resistance in salmon (Nichols et al. 2003), resistant trait to sea lice in the Atlantic salmon population (Tsai et al. 2016), expressed sequence tags from the ciliate protozoan parasite (Abernathy et al. 2007), and genetic analysis of resistant traits of *Columnaris* and *Edwardsiella ictaluri* in catfish (Zhou et al. 2017; Geng et al. 2015). Thus, it is vital to uncover the molecular markers that genetically linked to disease resistance and subsequently apply marker-assisted selection to expedite selection programs. Traditionally, quantitative trait loci (QTL) mapping with a dense genetic linkage map is an effective approach for dissecting important traits and developing genetically linked markers for selective breeding. In the genomic era, many high-throughput genotyping technologies have been developed, and the genome-wide association study (GWAS) becomes an efficient way for trait localization which does not require pedigree information or mapping family.

Linkage maps are essential tools for genomic and genetic studies, as well as for genetic breeding of economically important species (Peng et al. 2016). Recently, linkage maps have been constructed for many important teleost species including zebrafish (Bradley et al. 2011), medaka (Naruse et al. 2000), catfish (Kucuktas et al. 2009), tilapia (Liu et al. 2013), carps (Zhao et al. 2013; Zhang et al. 2013; Peng et al. 2016), Japanese flounder (Shao et al. 2015), and many others. Moreover, high-density genetic linkage maps provide a framework for QTL localization and facilitate genetic assistant selection and breeding in many aquaculture species (Zhou et al. 2018; Chen et al. 2018; Niu et al. 2017). For instance, growth-related traits have been mapped and fully investigated in many fishes, such as Pacific oyster (Song et al. 2018), catfish (Geng et al. 2017), and Asian seabass (Wang et al. 2015); sex determination traits have been localized in the genetic map in tilapia (Andrey et al. 2006), halibut (Palaiokostas et al. 2013), and Pacific white shrimp (Yu et al. 2017); oxygen tolerance in hybrid catfish (Zhong et al. 2017) and Nile tilapia (Li et al. 2017); salinity tolerance in tilapia (Gu et al. 2018; Lin et al. 2018); and resistance characters in red sea bream (Sawayama et al. 2017), Asian seabass (Wang et al. 2017), and so on.

To date, three draft genomes of the large yellow croaker have been published (Wu et al. 2014; Ao et al. 2015b) (PRJNA491413) and several versions of the large yellow croaker linkage maps have been constructed using various genetic markers including amplified fragment length polymorphism (AFLP), microsatellite, and single nucleotide polymorphism (SNP) markers (Ye et al. 2014; Ao et al. 2015a; Ning et al. 2007), and mapped some growth-related QTL and regions (Xiao et al. 2015). Additionally, a series of studies have been carried out on the life cycle of cryptocaryonosis, the expression and regulation of the anti-insect peptide piscidin, and the resistance gene of large yellow croaker (Ying et al. 2016; Zhou et al. 2014b). However, none of QTL analysis with challenge of *C. irritans*. Therefore, constructing a high-resolution genetic linkage map is vital for fine-scale mapping of cryptocaryonosis-resistant traits on genomic scale.

Here, we constructed a double-digest restriction-site associated DNA (ddRAD)-based high-density genetic map of the large yellow croaker. The map comprised 24 linkage groups with a total of 5261 SNP markers. Comparative genomic analysis with medaka, stickleback, European seabass and tilapia genomes provides us new insights of the synteny between *L. crocea* and models or Perciformes teleosts. We also identified QTL for *C. irritans* resistance trait on the linkage map, and the candidate genes were then identified from the genome regions of QTL intervals. Our high-density linkage map provides a powerful tool for QTL precise localization and association study of economically important traits, as well as a framework for assembling and improving reference genome of large yellow croaker.

Material and Methods

Mapping Family and DNA Extraction

A F1 full-sib family of large yellow croaker was generated from a maricultural farm (Ningde Fufa Aquatic Breeding Co.) in Ningde, Fujian, China. A total of 136 5-month progenies were randomly collected post hatch from the mapping family for genotyping and challenge experiment. The animal models were infected with a concentration of 2000 *C. irritans* theronts per fish in 3 L of seawater. Four days after infection, large numbers of tomonts were found to adhere to the bottom of aquarium. The fish were then transferred to another clean aquarium without tomonts. The time of death was recorded in the whole process of the experiment. Genomic DNA was extracted from the dorsal fins using the phenol-chloroform protocol (Sambrook et al. 1989). After quantification by a NanoDrop 2000 spectrophotometer (Thermo Scientific, Wilmington, DE, USA) and integrity detection by agarose gel electrophoresis, DNA samples were stored at − 20 °C for further experiments.

ddRAD Library Construction and Sequencing

Genomic DNA of 138 samples (2 parents and 136 offspring) was used to build ddRAD library. The ddRAD library was prepared using the improved published protocol (Peterson et al. 2012). Briefly, an equal amount of DNA (2 μg) of each sample was completely double digested with 20 units of *Eco*RI and *Msp*I. The reaction mixture was incubated at 37 °C for 13 h and 65 °C for 10 min. Then, the fragments were ligated with adaptors. The P1 adapter with forward amplification primer and barcode was added to the *Eco*RI overhang, and the P2 adapter with reverse amplification primer was added to the *Msp*I overhang, respectively. The ligation reaction was conducted in a reaction volume of 30 μl at 16 °C for 6 h on a thermocycler with a heated lid set to 65 °C for 10 min. After the heat kill, the solution was cooled down at 2 °C per 90 s until it reaches room temperature. After ligation, 24 individuals with different barcodes were pooled within one index, purifying with AMPure XP beads (Beckman Coulter, Brea, CA, USA). The DNA fragments of 300–400 bp were retrieved on E-Gel (Thermo Fisher Scientific) and then amplified with 30 cycles of PCR with regular forward primer and indexes ligated with reverse primer. Finally, six ddRAD libraries were sequenced on the Illumina HiSeq-PE150 platform with a 150-bp paired-end strategy at Novogene Technology (Tianjin, China).

SNP Discovery and Genotyping

The raw reads were first de-multiplexed according to the specific barcode-index combination of each sample. Reads with low quality and with ambiguous bases were discarded and trimmed to 130 bp because a slight increase of sequencing errors was observed after 130 bp. The cleaned data was filtered using Stacks v1.37 (Catchen et al. 2013). Firstly, we used *process_radtags* to distinguish individuals and chose BWA to align with the *L. crocea* genome. The *L. crocea* genome was our newly resequenced and assembled chromosome-level reference genome (BioProject: PRJNA505758). Secondly, stacks were constructed for each sample with *pstacks* (−*m*, 5). All individuals were then used to construct a catalog of loci using *cstacks*. The program *sstacks* (−*P*, 8) was used for matching against the catalog. Finally, the program *populations* was used for genotyping and only a genotype of the best SNP of each tag was used for further analysis.

The VCF file generated from *populations* was extracted and converted to Ped/Map format that served as an input file to PLINK software. All individuals with missing SNP genotypes (> 25%) and minor allele frequency (< 5%) were removed using the "–geno" and "–maf" parameters and manually removed with the low genome coverage. Internal Perl scripts were used for data cleaning. Only the SNPs that were heterozygous in at least one parent and in accordance with the Mendelian inheritance were used for further linkage analysis.

Linkage Map Construction

A genetic linkage map was constructed using JoinMap 4.1 software (Van Ooijen 2011) with *CP*-type population, which is designed to handle F1 population data containing two various heterozygous and homozygous diploid parents. The logarithm of odds (LOD = 19.0) was used for distributing SNP markers to different linkage groups (LGs). The recombination frequency of the same LG markers was transformed into map distance (cM) via the Kosambi mapping method (Kosambi 1943) in the regression algorithm. All genetic linkage maps were drawn using MapChart (Voorrips 2002).

Comparative Genomic Analysis

Comparative genomics was analyzed between large yellow croaker and each of the two perciforms, European seabass (*Dicentrarchus labrax*) and Nile tilapia (*Oreochromis niloticus*), as well as between large yellow croaker and each of the two model teleost species, medaka (*Oryzias latipes*) and stickleback (*Gasterosteus aculeatus*). Here, we used our newly assembled chromosome-level reference genome of *L. crocea* (BioProject No. PRJNA505758) and the four closely related species were downloaded from NCBI databases (https://www.ncbi.nlm.nih.gov/genome). The mapping and alignment were conducted using ddRAD tags with an *e* value cutoff of $1e^{-5}$ using BLASTN (Zhang et al. 2000). Among all the results obtained, we extracted non-overlapping sequences, each of which showed the lowest *e* value and the longest sequence length among the hits to a given region. There were no special requirements for the linkage group and chromosome number. Finally, syntenic regions defined by the top hits of the homology search were visualized using the program Circos v0.67 (Krzywinski and Schein 2009).

QTL Mapping Analysis and Association Study of Disease-Resistant Traits

QTL mapping with death time phenotypes was performed using the MapQTL6 software package (Van Ooijen 2011) with *composite interval mapping* (IM) and *restricted multiple QTL model (MQM) mapping* algorithms. LOD score significance thresholds were calculated by 1500 permutation tests for the trait. The genome-wide LOD threshold at a P value < 0.05 was considered to be significant. As a complementary method for QTL mapping, the genome-wide association study was performed between genotypes and traits using genome-wide efficient mixed model association (GEMMA) (Zhou and

Stephens 2012) with a univariate linear mixed model (LMM) of phenotype on genotype. Combining the results from both QTL mapping and association analysis, we identified SNP loci that significantly correlated with the traits and extracted candidate genes cross these SNP loci to identify candidate genes associated with cryptocaryonosis-resistant traits. Briefly, we screened the ± 50,000-bp genome regions surrounding the significant SNPs based on the *L. crocea* reference genome and annotated the candidate genes accurately by BLAST against the non-redundant protein database.

Results

ddRAD-Seq Library Construction and SNP Quality Control

A total of 6 ddRAD sequencing (ddRAD-seq) libraries from 2 parents and their 136 offspring were constructed and sequenced by the HiSeq PE150 platform (BioProject No. PRJNA513258). After trimming, filtering the lower quality reads, assessing the genotyping quality, and removing samples according to sequencing mean depth (< 25), a total of 109,503 SNP markers were obtained from 2 parents and 124 progenies. Then, we continue to filter the SNPs with missing SNP genotypes (> 25%) and minor allele frequency (< 5%), and a total of 30,540 SNP markers were retained for linkage analysis. According to the Mendelian inheritance together with all tags which only hold the single version, 6226 SNPs were heterozygous in either one of the parents and were genotyped for adequate numbers of progeny (Supplementary File). Finally, only 5261 SNP markers were used for constructing the linkage map based on the LOD threshold. Details of each sample are shown in Table S1.

High-Density Genetic Map Construction

A high-density ddRAD-based SNP genetic map of large yellow croaker based on a pseudo-testcross population was constructed using JoinMap 4.1. The remaining putative 5261 SNPs were successfully grouped into 24 LGs (Table 1, Fig. 1). The total genetic map length was 1885.67 cM with an average LG that contained 219 effective loci spanning 78.570 cM. Specifically, LG3 had the most numbers of loci spanning 119.994 cM, whereas LG23 had the least number of effective loci spanning 61.092 cM. The inter-locus distance estimated based on the unique marker positions ranged from 0.25 cM in LG6 to 0.50 cM in LG24 with an average inter-locus distance of 0.36 cM in the map. Details of SNP names and positions on the 24 LGs of the integrated genetic map are listed in Table S2.

Comparative Genomics

The high-density linkage map represented a valuable resource for future comparative genome analysis with closely related model fishes. We repasted the similarity of loci (1.0) filtered from JoinMap 4.1 onto the corresponding SNP chromosome and eventually obtained 5755 SNPs. The *loci (1.0)* meant that the two SNPs were completely consistent in all individuals. To compare chromosome framework among teleosts, we used the 5755 ddRAD tags searched against the chromosomes of medaka, stickleback, European seabass, and tilapia. The Circos plots were drawn based on the ortholog pairs between four species.

For comparison of the croaker-medaka and croaker-European seabass, 878 (15.27%) and 3277 (56.94%) of 5755 1:1 best ortholog pairs had been mapped on those paired chromosomes (Fig. 2a, b), respectively. Although we observed that parts of the large yellow croaker LGs correspond to several chromosomes in medaka or seabass, the major markers in the croaker chromosomes tended to be represented in only one corresponding chromosome, which built perfect chromosome-scale syntenic boxes.

Similarly, comparative genomic analysis was also performed between croaker and stickleback genomes. A total of 1423 (24.73%) 1:1 best ortholog pairs were identified. The comparison between the croaker and stickleback (Fig. 2c) revealed that 18 of the 24 croaker chromosomes have chromosome-level conserved syntenic blocks with stickleback chromosomes. Except the 1:1 correspondence of chromosomes in the two species, we also identified the portion 2:1 chromosome relationship between croaker and stickleback. Chromosome 1 of stickleback ortholog occurred in croaker linkage groups LG13 and LG18. Likewise, stickleback chromosome 4 was examined to be co-orthologous to croaker LG7 and LG23 as well as to croaker LG10 and LG24 orthologs, which were distributed in stickleback chromosome 7. This interesting 1:2 synteny suggested that the chromosome fusion events might occur post the divergence of croaker and gasterosteus.

Moreover, comparative genomic analysis of large yellow croaker with tilapia was also performed, which revealed that a total of 1914 (33.26%) 1:1 best ortholog pairs were dentified in tilapia (Fig. 2d). The extensive syntenic blocks were quite obviously for some chromosomes/linkage pairs, e.g., LC_LG1-ON_chr6, LC_LG2-ON_chr8, and LC_LG21-ON_chr13, but there were also few exceptions in conditions of the croaker linkage group. The croaker LG4 was made of two corresponding tilapia chromosomes ON_chr17 and ON_chr23. Conversely, LC_LG17 and LC_LG20 was mainly syntenically related to one tilapia linkage group, ON_chr7. This syntenic pattern would imply at least three inter-chromosomal rearrangements between the two species.

Table 1 Characteristics of the genetic map of the large yellow croaker

LG	No. of SNPs	Marked loci	Distance (cM)	Average inter-locus distance (cM)
LG1	231	229	66.631	0.29
LG2	221	220	92.134	0.42
LG3	270	268	119.994	0.45
LG4	263	262	78.602	0.30
LG5	259	257	82.938	0.32
LG6	261	259	65.155	0.25
LG7	224	222	73.113	0.33
LG8	234	233	86.093	0.37
LG9	207	204	94.382	0.46
LG10	246	245	82.991	0.34
LG11	246	245	85.727	0.35
LG12	236	230	61.450	0.27
LG13	224	221	66.012	0.30
LG14	227	225	87.949	0.39
LG15	222	222	102.417	0.46
LG16	219	216	70.033	0.32
LG17	217	216	82.420	0.38
LG18	214	213	77.468	0.36
LG19	204	203	73.160	0.36
LG20	203	200	91.121	0.46
LG21	165	162	61.742	0.38
LG22	185	184	61.450	0.33
LG23	158	158	61.092	0.39
LG24	125	123	61.596	0.50
Total	5261	5217	1885.670	0.36

Fine Mapping of QTL and Related Genes for Disease-Resistant Traits

We employed restricted MQM mapping to detect QTLs for resistant traits. The data of death time is shown in Table S3. Because of the small sample size, our phenotype distribution could not accurately satisfy the Gaussian mixture model. This was a preliminary result, and for the complex traits of *C. irritans* resistance, large samples were needed for more accurate QTL mapping. In general, seven significant QTLs under *C. irritans* challenge were distributed on LG5, LG6, LG7, and LG19 of large yellow croaker (Table 2 and Fig. 3). The most significant QTL CIR-5 located on LG19 at 26.640–26.902 cM presented the highest LOD value of 13.69, explaining the highest percentage of the phenotypic variations (32.7%). Another QTL CIR-6 and CIR-7 on LG19 were detected at position 65.201–66.877 with LOD values of 9.56–11.41 and contributions to a phenotypic variation of 32.1–32.4%. On LG5, CIR-1 and CIR-2 were located at 25.118–25.718 cM and 62.835–63.934 cM, explaining a 23.3–24.5% phenotypic variation. The QTL CIR-3 located on LG6 at 50.395–51.885 cM explained the lowest percentage of the phenotypic variations (3.1%) with a LOD value of 7.64 while QTL CIR-4 located on LG7 at 30.555–30.564 cM explained 30.8% of the total phenotypic variations with a LOD value of 7.43. We also conducted genome-wide association analysis between SNP genotypes and *C. irritans* challenge phenotypes as a complementary. The results revealed similar distribution patterns with QTL mappings. Integrating the results of both approaches, we certified that the identified SNP loci were significantly associated with disease-related traits.

Several genes related to disease resistance were identified from QTL mapping of the high-density map based on the large yellow croaker genome annotation. A total of 36 genes (Supplementary Table S4) were identified from the QTL regions, of which 29 (Table 3) were immune or disease-related genes, such as *inhibitor of nuclear factor kappa-B kinase subunit epsilon* (*ikbke*), *nectin-2* (*CD112*), *interferon alpha/beta receptor 1* (*ifnar1*), and *interferon gamma receptor 2* (*ifngr2*). Inhibitor of nuclear factor kappa-B kinase subunit epsilon (IKBKE) is a non-canonical member of the IκB kinase (IKK) family and regulates immune response (Shih et al. 2011), which is identified on LG5 (Fig. 4a). Further, we identified *nectin-2* on LG6 (Fig. 4b) which were immunoglobulin

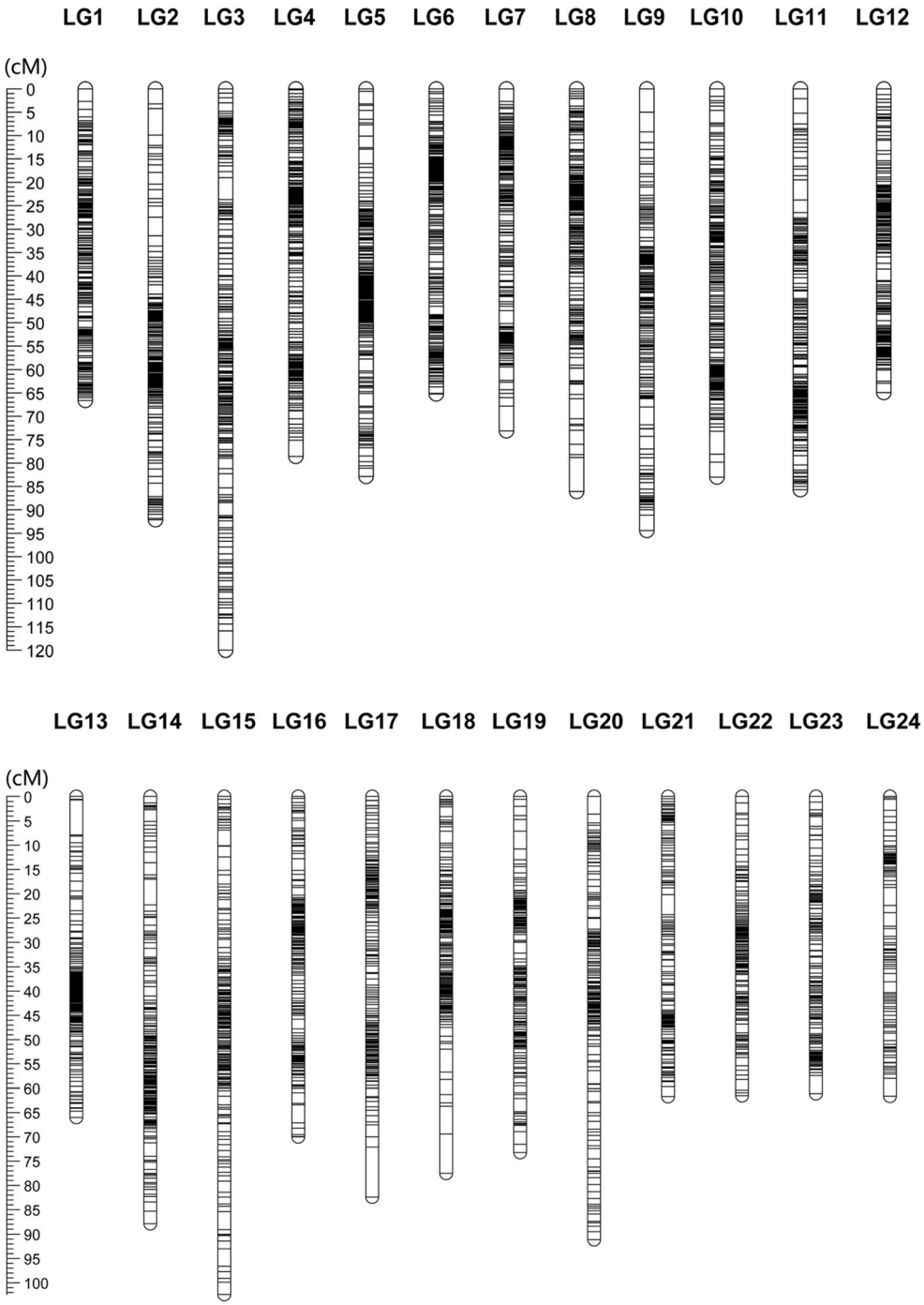

Fig. 1 The high-density consensus linkage genetic map for large yellow croaker

(Ig)-like cell adhesion molecules (CAMs) that play key roles in a variety of the formation of cell-cell adhesions and novel regulators of cellular activities, including cell polarization, differentiation, movement, proliferation, and survival (Takai et al. 2008). Interferon receptors (*ifnrs*) were located on QTL CIR-7 of LG19 (Fig. 4c) and belonged to the class II helical cytokine receptor family (*CRF2*) which could activate the responsive elements in the nucleus and induce the transcription and expression of antiviral proteins, playing an important role in regulating the immune response against foreign pathogens (Zhou et al. 2014a; Krause and Pestka 2005). Finally, the information on the mechanisms of *ifnr*, *ikbke*, and *nectin-2* actions against *C. irritans* is visualized in Fig. 5.

Discussion

Genetic maps which were constructed using sequence-based SNP markers were useful in genetic studies including comparative genomics, functional gene mapping, candidate gene

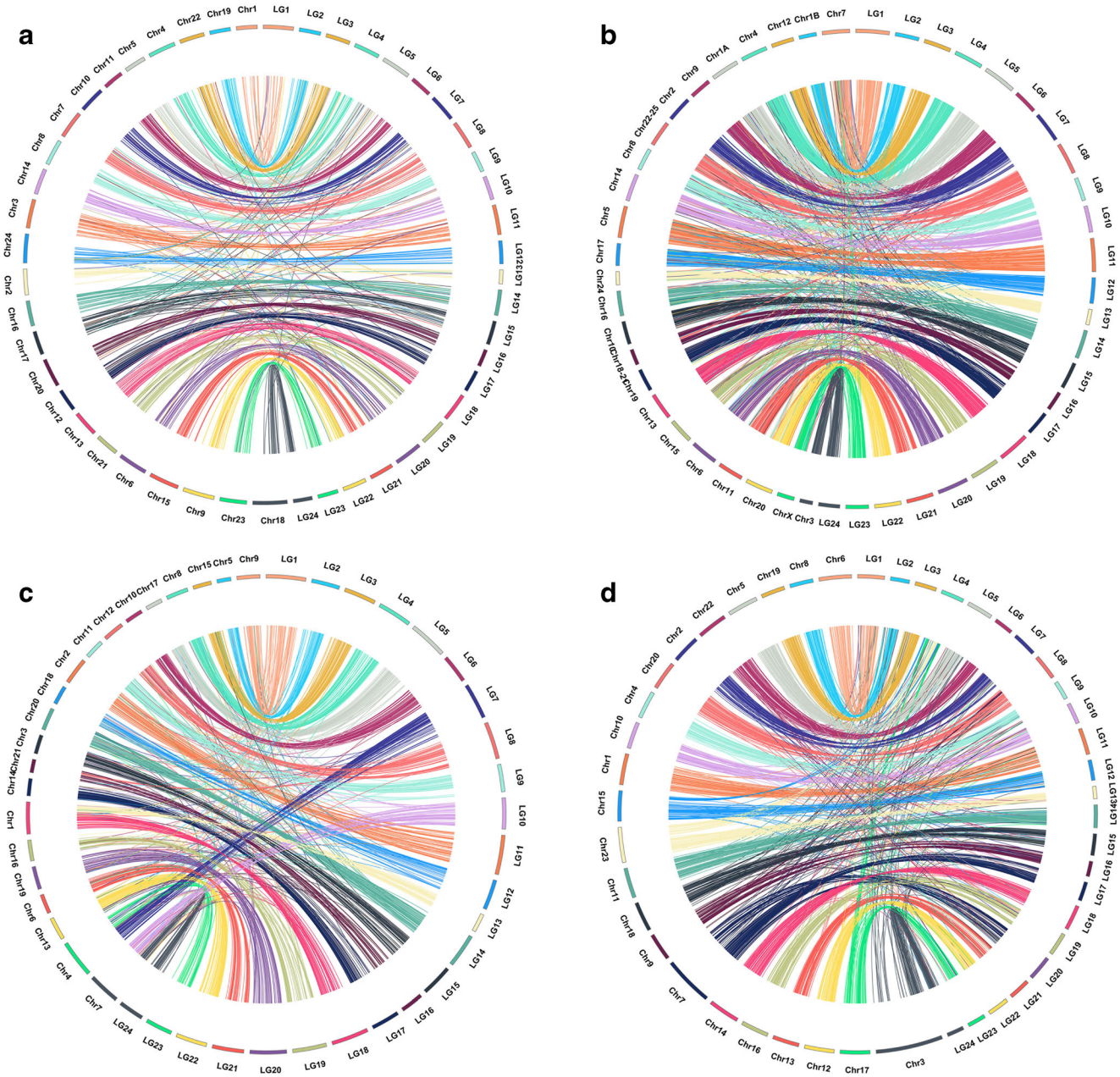

Fig. 2 Genomic comparisons as shown by the Circos diagram between large yellow croaker and medaka (**a**), European seabass (**b**), stickleback (**c**), and tilapia (**d**). Each colored arc represents an orthologous match between two species. We messed up the order of the four closely related species genome chromosomes on the image to better illustrate our results

positional cloning, and genome assembly (Kujur et al. 2015; Yue 2014; Xu et al. 2014a). Linkage maps have been constructed for many important aquaculture species since the first report of the linkage map of tilapia in 1998 (Kocher et al. 1998). To date, SNPs are a particularly attractive approach for genetic map construction due to the most common type of DNA polymorphism in the genome (Berthier-Schaad et al. 2010). With the progress of the next-generation sequencing technologies, various sequence-based SNP genotyping technologies have been detected, providing rapid and cost-effective high-throughput SNP genotyping platforms for linkage mapping. Additionally, RAD sequencing approaches come into vogue for linkage mapping in non-model species (Gonen et al. 2014; Shao et al. 2015; Le et al. 2015). In the present study, we used the ddRAD-seq approach to discover and genotype SNPs in large yellow croaker. Among the identified SNPs, 5261 ddRAD-based SNP markers were successfully genotyped and assigned to 24 LGs corresponding to the 24 chromosome pairs of the genome. The total length of the linkage map was 1885.67 cM with an average marker interval of 0.36 cM. Many genetic maps of large yellow croaker have been previously constructed using various markers, but the

Table 2 Summary of the *C. irritans* disease resistance QTLs in large yellow croaker

QTL name	LG	Genetic position (cM)	No. of SNPs	LOD	Exp%	Nearest marker
CIR-1	5	25.118–25.718	1	8.66	23.3	snp3839_112
CIR-2	5	62.835–63.934	3	11.65	24.5	snp27493_90
CIR-3	6	50.395–50.885	1	7.64	3.1	snp24659_109
CIR-4	7	30.555–30.564	1	7.43	30.8	snp42162_7
CIR-5	19	26.640–26.902	2	13.69	32.7	snp33090_20
CIR-6	19	65.201–65.601	1	11.41	32.4	snp14459_104
CIR-7	19	66.377–66.877	1	9.56	32.1	snp21321_36

Exp% percentage of the explained phenotypic variation

density of the maps varies considerably. Our new map was the first ultra-high-density linkage map, representing a significant improvement over the previous linkage maps constructed by microsatellite markers (0.76 cM) (Ye et al. 2014) and RAD-based SNP markers (0.54 cM) (Ao et al. 2015a), although the method (Lep-MAP (Rastas et al. 2013) vs JoinMap 4.1) and data type (SNP vs microsatellite) were different.

Comparative genomics is a powerful tool to transfer genomic information from model species to related non-model species. Teleost-specific genome duplication and accompanying genome rearrangements were reported to lead to teleost species with a higher rate of gene linkage disruption and lineage divergence than mammals (Kasahara et al. 2007; Meyer and Van de Peer 2005). Whole-genome duplication (WGD) and subsequent asymmetric changes in duplicated genes were thought to have an important role in genome evolution (Xu et al. 2014b). In a relatively short period of ~ 50 Myr after the WGD event (336~404 Myr ago), the MTZ ancestor (the last common ancestor of medaka, *Tetraodon*, and zebrafish) had 24 chromosomes and undergone 8 major inter-chromosomal rearrangements (2 fissions, 4 fusions, and 2 translocations) and only the medaka genome has preserved its ancestral genomic structure without undergoing major inter-chromosomal rearrangements for more than 300 Myr (Kasahara et al. 2007; Takeda 2008). In our study, we performed the chromosome-level comparisons between the croaker and two model species, medaka and stickleback. The results provided evidence that the croaker genome is more closely related to the medaka genome than the genome of stickleback. The comparison between the croaker and European seabass indicated that their chromosomes present 1:1 chromosome-level syntenic blocks, suggesting their close phylogenic relationship in perciforms.

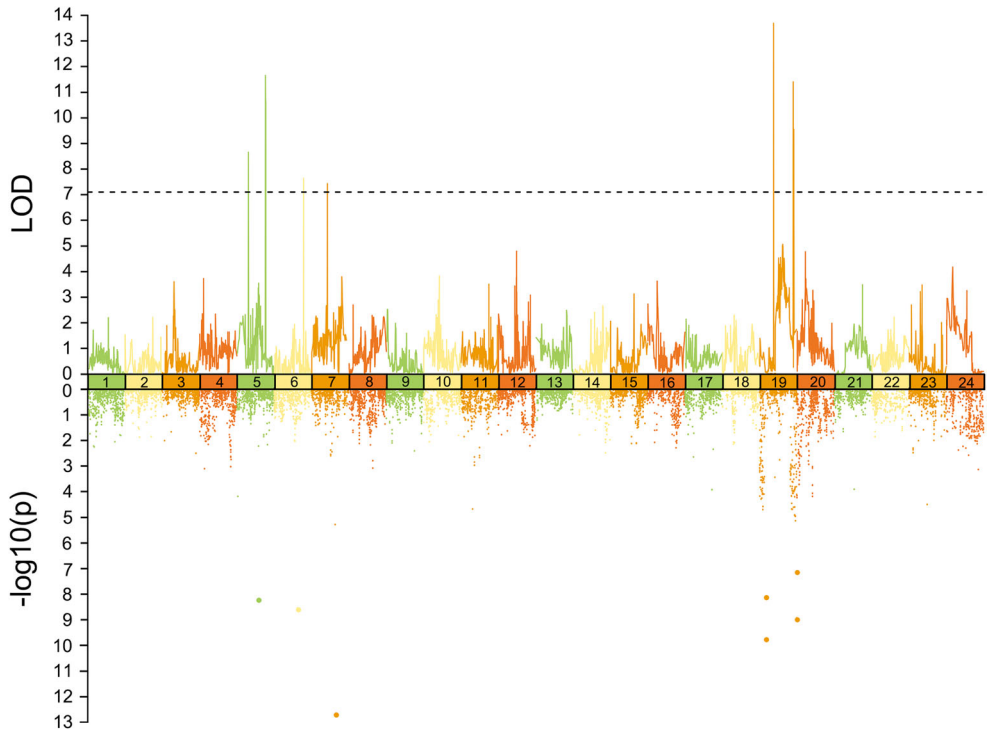

Fig. 3 QTL mapping and associate analysis of *C. irritans* resistance traits in large yellow croaker. The black horizontal line represents the genome-wide significance threshold where logarithm of odds (LOD) was 7.1

Table 3 Summary of the candidate genes from QTLs in large yellow croaker

QTL	LG	Gene name	Annotation
CIR-1	LG5	*rassf5*	Ras association domain-containing protein 5
		ikbke	Inhibitor of nuclear factor kappa-B kinase subunit epsilon
		fam72a	Protein FAM72A
CIR-2	LG5	*mct2*	Monocarboxylate transporter 2
		lrig1	Leucine-rich repeats and immunoglobulin-like domain protein 1
		slc25a26	*S*-Adenosylmethionine mitochondrial carrier protein
		adamts1	A disintegrin and metalloproteinase with thrombospondin motif 9
CIR-3	LG6	*cd112*	Nectin-2
CIR-4	LG7	*commd5*	COMM domain-containing protein 5
		fam199x	Protein FAM199X
		nek1	Serine/threonine-protein kinase Nek1
		smim19	Small integral membrane protein 19
		pld3	Phospholipase D3
		gpr137	Integral membrane protein GPR137
		syvnl	E3 ubiquitin-protein ligase synoviolin
		hdac3	Histone deacetylase 3
		myot	Myotilin
CIR-5	LG19	*fbxo47*	F-box only protein 47
		arl6	ADP-ribosylation factor-like protein 6
		arp3	Actin-related protein 3
		ddx18	ATP-dependent RNA helicase DDX18
		ube2f	NEDD8-conjugating enzyme UBE2F
		sprysec7	SPRY domain-containing protein 7
CIR-6	LG19	*trim13*	Tripartite motif-containing 13
		rnaseh2b	Ribonuclease H2 subunit B
		gucy1b2	Guanylate cyclase soluble subunit beta-2
CIR-7	LG19	*ifnar1*	Interferon-alpha/beta receptor 1a
		ifngr2	Interferon-gamma receptor 2 precursor
		tmem50b	Transmembrane protein 50B

In contrast, 2:1 syntenic correspondences were found in large yellow croaker linkage groups with stickleback (21) (Peichel et al. 2001) and tilapia (22) (Guyon et al. 2012), indicating that dramatic genome rearrangements occurred after these species diverged. This observation of a few exceptions of the 2:1 phenomenon suggests the genome plasticity and the underlying evolutionary constraints may not be evenly distributed across the genome, as large yellow croakers LG13 and LG23 both undergo inter-chromosomal rearrangements in stickleback and tilapia. Meanwhile, large-scale chromosomal rearrangements were rare but small fusion and translocations were subsistent. Moreover, all linkage groups in large yellow croaker mainly corresponded to one or two chromosomes in the four model fishes (Fig. 2), implying the high evolutionary conservation of chromosomes in these five species. Finally, large yellow croaker linkage group 4 corresponded to two chromosomes in tilapia, suggested that the group may easily occur independent of chromosomal fission events. Our findings could facilitate the functional inference of genes in croaker and further benefit the studies of karyotype evolution in teleosts.

The availability of mapping QTL is to understand the numbers and effects of genes that determine the traits on the whole genome and to assist in selective breeding to accelerate genetic improvement of important traits. Disease resistance is one of the most important researched traits in QTL studies as diseases represent one of the major challenges and bottlenecks in aquaculture. In our study, we identified 29 immune- or disease-related genes. Interferons have been shown to be a potent regulator of adaptive immunity, which now becomes clear that a broad range of viruses, bacteria, and even parasites express ligands capable of stimulating a growing number of signal pathways that must be specifically bound to the corresponding interferon receptors in order to perform biological functions (Smith et al. 2005). Thus, interferon receptors as molecular switches play a decisive role in the host immune response. Interferon receptor knockout models have made significant contributions to elucidating their associated immune

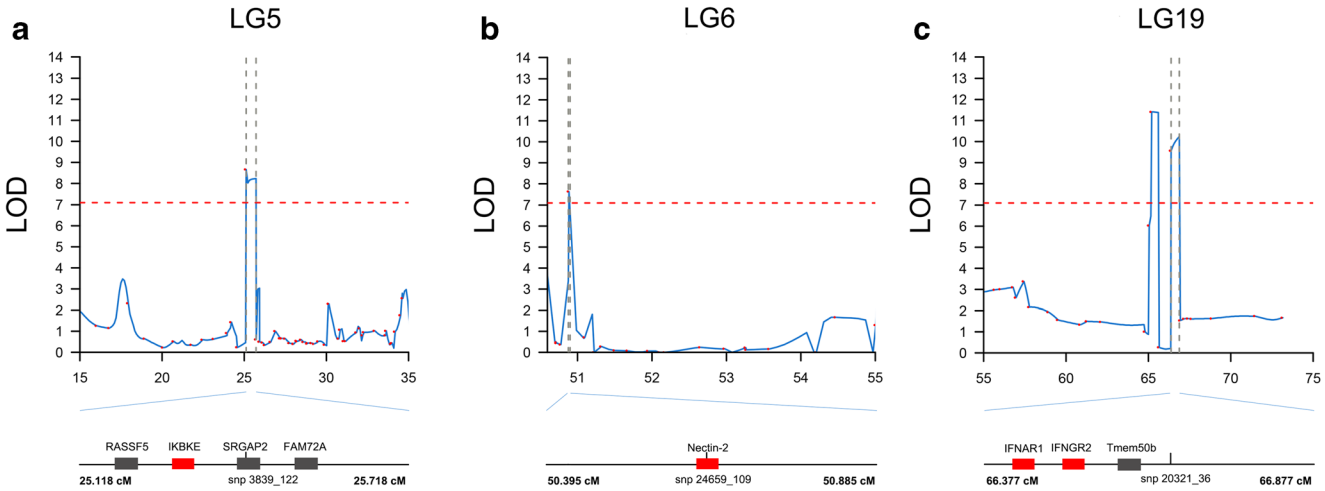

Fig. 4 **a**–**c** QTL region and candidate genes for *C. irritans* resistance traits in large yellow croaker. Genes are extracted in the ± 50,000-bp genome regions around the significant SNPs. Rectangles represent the candidate genes, and red rectangles were the highlighted genes

mechanisms in mice (Jabbar et al. 2013; De et al. 2013). Some studies showed interferons, especially type I interferons, have been described as the master factors that bridge innate and adaptive immunity (Ivashkiv and Donlin 2014; Schoggins et al. 2010); clearly, the *ifnar1* functions as the signal locks. In addition, disruption of interferon (IFN) or its receptor causes increased susceptibility to viral, bacterial, and parasitic infections in animal models (Smith et al. 2005). A study found IFN-gamma receptor null-mutant mice were more susceptible to herpes simplex virus type 1 infection than IFN-gamma

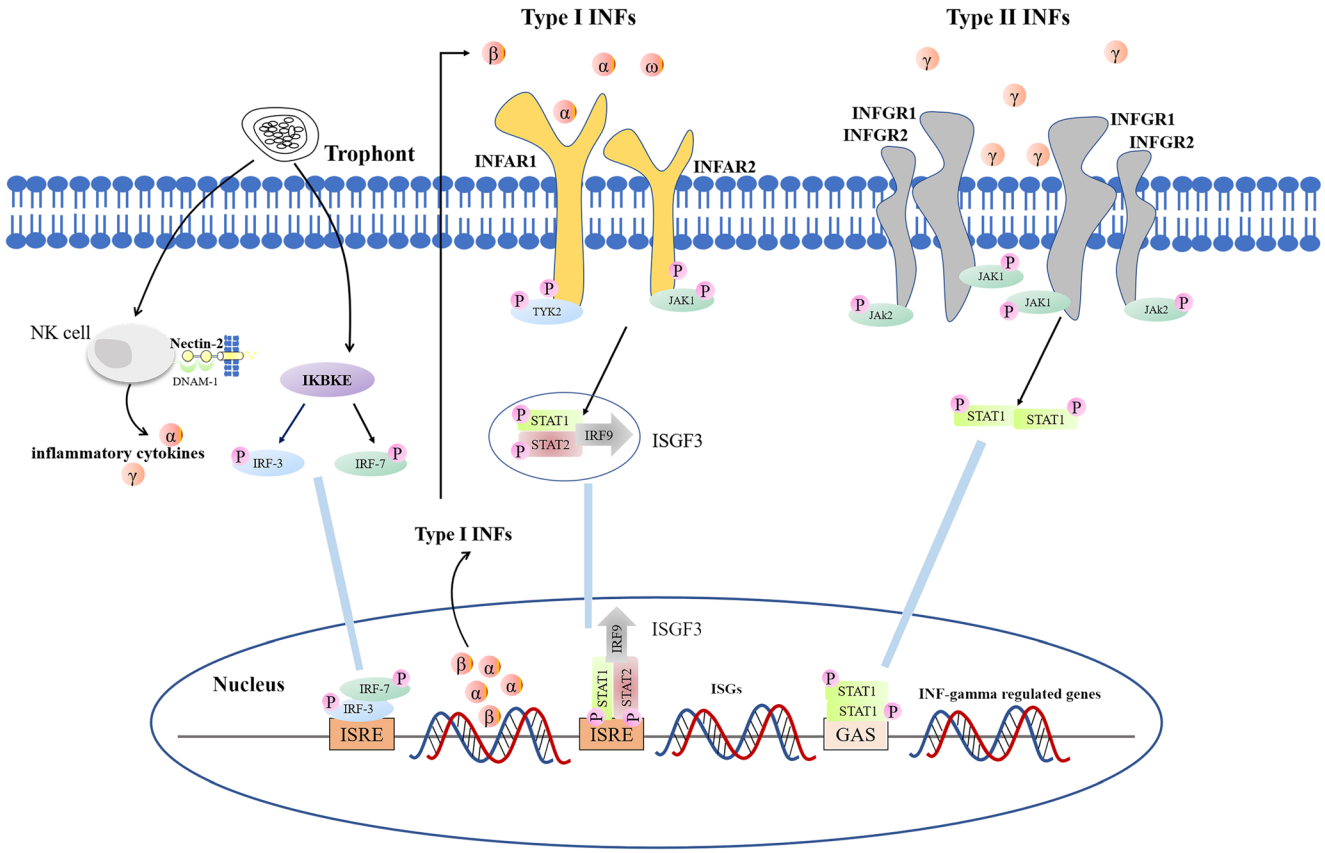

Fig. 5 Pathways of *interferon receptor*, *inhibitor of nuclear factor kappa-B kinase subunit epsilon*, and *nectin-2* induction and effect in *C. irritans* infection. When *C. irritans* infect, NK cell with *DNAM-1* and *nectin-2* produce high levels of inflammatory cytokines, while *ikbke* promotes phosphorylation of interferon (*ifn*) regulatory factor 3 (*irf3*) and *irf7* which bind to the response elements, eventually promoting expression of type I *ifn* genes. Type I *ifns* bind to respective receptors, activate the JAK-STAT pathway, and then induce the overlapping ISGs. IFN-γ activates STAT1 and induces a partially overlapping but distinct ISGs

ligand null-mutant mice (Cantin et al. 1999). Herpes simplex virus is a common human infectious skin disease, and after infection *C. irritans*, large yellow croaker also had the largest skin damage, which demonstrated the importance and reliability of the candidate gene. Interestingly, when fish is infected with *C. irritans*, interferon as one of the second lines of defense against pathogens may rapidly eliminate invasive parasites. Also, interferon binding to interferon receptors could trigger the induction of the expression of hundreds of IFN-inducible genes via the Janus kinase (JAK) and signal transduction and activators of transcription (STAT) signaling pathway (Sun et al. 2014). Additionally, in response to inflammatory factor and viral infection, *IKBKE* was activated and subsequently phosphorylates interferon response factors 3 and 7 (*IRF3* and *IRF7*, respectively) and signal transducer and activator of transcription 1 (STAT1) (tenOever et al. 2007), this suggest *ikbke* and *ifn* may interact. Moreover, nectin-2 has some other important biological functions besides the structure features of an extracellular region with three Ig-like loops, a single transmembrane region, a cytoplasmic tail region (Takai et al. 2008), and cell adhesion functions, and it was also an important immune molecule. Some studies showed nectin-2 could activate the activity of natural killer (NK) cells and trigger a variety of immunological effects, including graft rejection, virus infection defense, and killing of tumor cells (Taharahanaoka et al. 2006; Baury et al. 2003). However, there were no reports about the functional domains and precise sites. Further studies stated nectin-2 has been identified as a ligand of DNAX accessory molecule 1 (DNAM-1) in both humans and mice (Taharahanaoka et al. 2005; Pende et al. 2005). Evidence from in vitro and in vivo studies revealed that the interaction of DNAM-1 with its ligands is involved in the functions of a variety of immune cells (Iguchimanaka et al. 2008; Gilfillan et al. 2008), so nectin-2 also plays an important role in immune cells. Nectin-2 was expressed in blood cells (Mori et al. 2014) and epithelial cells (Takai et al. 2008), and it may form a stable barrier on the surface of the skin through the cell-cell adhesion system to prevent the invasion of *C. irritans* or play roles in transient cell-cell contacts, such as those between macrophages and lymphocytes and between leukocytes and vascular endothelial cells, but the exact roles of nectin-2 in blood cells remain unknown.

Overall, our results provided some immune-associated SNP markers, which will facilitate the molecular marker-assisted selection design of resistant populations of large yellow croaker. Also, further verification of functional experiments of the mapped genes in this study is necessary.

Conclusions

Here, a high-density genetic linkage map was constructed with 5261 SNPs using the ddRAD-seq approach. The map consisted of 24 linkage groups, spanning 1885.67 cM with an average marker interval of 0.36 cM. Comparative genomic analyses have been conducted between large yellow croaker and four closely related species, indicating that high evolutionary conservation of chromosomes existed in these fish species as well as inter-chromosomal rearrangements with certain fusion, translocation, or fission events. Through SNP mapping analysis, we identified seven significant QTLs under *C. irritans* challenge and functional genes underlying these traits, which will be significant to improve breeding in large yellow croaker. Our work provides excellent useful genomic resources for the improvement of genome sequence assembly and molecular dissection of disease resistance, and lays a foundation in the future for molecular assisted breeding of new varieties of *C. irritans* resistance of large yellow croaker.

Author Contributions PX conceived of the project. PX contributed to the funding acquisition. SK wrote the manuscript. SK, LC, and WP performed the analysis and designed the charts and tables. QK, JZ, and HB conducted the *C. irritans* challenge experiment. ZZ and FP conducted the ddRAD libraries. All authors have validated the manuscript and appreciate to improve the quality of it.

Funding Information We acknowledge the financial support from the State Key Laboratory of Large Yellow Croaker Breeding (Fujian Fuding Seagull Fishing Food Co., Ltd.) (LYC2017RS05 and LYC2017ZY01), the Fundamental Research Funds for the Central Universities of Xiamen University (Nos. 20720180123 and 20720160110), the Science and Technology Platform Construction of Fujian Province (No. 2018 N2005), the Local Science and Technology Development Project Guide by The Central Government (2017L3019), and the Natural Science Foundation of Fujian Province (Grant No. 2017 J06022).

Compliance with Ethical Standards

Conflict of Interest The authors declare that they have no conflict of interests.

References

Abernathy JW, Xu P, Li P, Xu D-H, Kucuktas H, Klesius P, Arias C, Liu Z (2007) Generation and analysis of expressed sequence tags from the ciliate protozoan parasite Ichthyophthirius multifiliis. BMC Genomics 8:176

Andrey S, Eyal S, Avner C, Howe AE, Raisa D, Noam Z, Kocher TD, Gideon H, Micha R (2006) Amh and Dmrta2 genes map to tilapia (*Oreochromis* spp.) linkage group 23 within quantitative trait locus regions for sex determination. Genetics 174:1573–1581

Ao J, Li J, You X, Mu Y, Ding Y, Mao K, Bian C, Mu P, Shi Q, Chen X (2015a) Construction of the high-density genetic linkage map and chromosome map of large yellow croaker (*Larimichthys crocea*). Int J Mol Sci 16:26237–26248

Ao J, Mu Y, Xiang L-X, Fan D, Feng M, Zhang S, Shi Q, Zhu L-Y, Li T, Ding Y, Nie L, Li Q, Dong W-R, Jiang L, Sun B, Zhang X, Li M, Zhang H-Q, Xie S, Zhu Y, Jiang X, Wang X, Mu P, Chen W, Yue Z,

Wang Z, Wang J, Shao J-Z, Chen X (2015b) Genome sequencing of the perciform fish *Larimichthys crocea* provides insights into molecular and genetic mechanisms of stress adaptation. PLoS Genet 11: e1005118

Baury B, Masson D, Mcdermott BM, Jarry A, Blottière HM, Blanchardie P, Laboisse CL, Lustenberger P, Racaniello VR, Denis MG (2003) Identification of secreted CD155 isoforms. Biochem Biophys Res Commun 309:175–182

Berthier-Schaad Y, Kao WHL, Coresh J, Zhang L, Ingersoll RG, Stephens R, Smith MW (2010) Reliability of high-throughput genotyping of whole genome amplified DNA in SNP genotyping studies. Electrophoresis 28:2812–2817

Bradley KM, Breyer JP, Melville DB, Broman KW, Knapik EW, Smith JR (2011) An SNP-based linkage map for zebrafish reveals sex determination loci. G3 (Bethesda) 1:3–9

Cantin E, Tanamachi B, Openshaw H, Mann J, Clarke K (1999) Gamma interferon (IFN-gamma) receptor null-mutant mice are more susceptible to herpes simplex virus type 1 infection than IFN-gamma ligand null-mutant mice. J Virol 73:5196–5200

Catchen J, Hohenlohe PA, Bassham S, Amores A, Cresko WA (2013) Stacks: an analysis tool set for population genomics. Mol Ecol 22: 3124–3140

Chen L, Peng W, Kong S, Pu F, Chen B, Zhou Z, Feng J, Li X, Xu P (2018) Genetic mapping of head size related traits in common carp (*Cyprinus carpio*). Front Genet 9. https://doi.org/10.3389/fgene.2018.00448

De LPF, Calvopinilla E, López gil E, Marínlópez A, Mateos F, Castilloolivares J, Lorenzo G, Ortego J (2013) Ns1 is a key protein in the vaccine composition to protect Ifnar(-/-) mice against infection with multiple serotypes of African horse sickness virus. PLoS One 8:e70197

Fuji K, Hasegawa O, Honda K, Kumasaka K, Sakamoto T, Okamoto N (2007) Marker-assisted breeding of a lymphocystis disease-resistant Japanese flounder (*Paralichthys olivaceus*). Aquaculture 272:291–295

Geng X, Sha J, Liu S, Bao L, Zhang J, Wang R, Yao J, Li C, Feng J, Sun F, Sun L, Jiang C, Zhang Y, Chen A, Dunham R, Zhi D, Liu Z (2015) A genome-wide association study in catfish reveals the presence of functional hubs of related genes within QTLs for columnaris disease resistance. BMC Genomics 16:196

Geng X, Liu S, Yuan Z, Jiang Y, Zhi D, Liu Z (2017) A genome-wide association study reveals that genes with functions for bone development are associated with body conformation in catfish. Mar Biotechnol 19:570–578

Gilfillan S, Chan CJ, Cella M, Haynes NM, Rapaport AS, Boles KS, Andrews DM, Smyth MJ, Colonna M (2008) DNAM-1 promotes activation of cytotoxic lymphocytes by nonprofessional antigen-presenting cells and tumors. J Exp Med 205:2965–2973

Gonen S, Lowe NR, Cezard T, Gharbi K, Bishop SC, Houston RD (2014) Linkage maps of the Atlantic salmon (*Salmo salar*) genome derived from RAD sequencing. BMC Genomics 15:166

Gu XH, Jiang DL, Huang Y, Li BJ, Chen CH, Lin HR, Xia JH (2018) Identifying a major QTL associated with salinity tolerance in Nile Tilapia using QTL-Seq. Mar Biotechnol 20:98–107

Guyon R, Rakotomanga M, Azzouzi N, Coutanceau JP, Bonillo C, D'cotta H, Pepey E, Soler L, Rodier-Goud M, D'hont A (2012) A high-resolution map of the Nile tilapia genome: a resource for studying cichlids and other percomorphs. BMC Genomics 13:222–222

Iguchimanaka A, Kai H, Yamashita Y, Kai S, Taharahanaoka S, Honda S, Yasui T, Kikutani H, Shibuya K, Shibuya A (2008) Accelerated tumor growth in mice deficient in DNAM-1 receptor. J Exp Med 205:2959–2964

Ivashkiv LB, Donlin LT (2014) Regulation of type I interferon responses. Nat Rev Immunol 14:36–49

Jabbar TK, Calvo-Pinilla E, Mateos F, Gubbins S, Bin-Tarif A, Bachanek-Bankowska K, Alpar O, Ortego J, Takamatsu HH, Mertens PP (2013) Protection of IFNAR (-/-) mice against bluetongue virus serotype 8, by heterologous (DNA/rMVA) and homologous (rMVA/rMVA) vaccination, expressing outer-capsid protein VP2. PLoS One 8:e60574

Jian J, Wu Z (2003) Effects of traditional Chinese medicine on nonspecific immunity and disease resistance of large yellow croaker, Pseudosciaena crocea (*Richardson*). Aquaculture 218:1–9

Kasahara M, Naruse K, Sasaki S, Nakatani Y, Qu W, Ahsan B, Yamada T, Nagayasu Y, Doi K, Kasai Y (2007) The medaka draft genome and insights into vertebrate genome evolution. Nature 447:714–719

Kocher TD, Lee WJ, Sobolewska H, Penman D, Mcandrew B (1998) A genetic linkage map of a cichlid fish, the tilapia (*Oreochromis niloticus*). Genetics 148:1225–1232

Kosambi DD (1943) The estimation of map distance from recombination values. Ann Eugenics 12:172–175

Krause CD, Pestka S (2005) Evolution of the class 2 cytokines and receptors, and discovery of new friends and relatives. Pharmacol Ther 106:299–346

Krzywinski M, Schein JI (2009) Circos: an information aesthetic for comparative genomics. Genome Res 19:1639–1645

Kucuktas H, Wang S, Li P, He C, Xu P, Sha Z, Liu H, Jiang Y, Baoprasertkul P, Somridhivej B (2009) Construction of genetic linkage maps and comparative genome analysis of catfish using gene-associated markers. Genetics 181:1649–1660

Kujur A, Upadhyaya HD, Shree T, Bajaj D, Das S, Saxena MS, Badoni S, Kumar V, Tripathi S, Gowda CL (2015) Ultra-high density intra-specific genetic linkage maps accelerate identification of functionally relevant molecular tags governing important agronomic traits in chickpea. Sci Rep 5:9468

Le W, Zi YW, Bai B, Shu QH, Chua E, Lee M, Hong YP, Yan FW, Peng L, Feng L (2015) Construction of a high-density linkage map and fine mapping of QTL for growth in Asian seabass. Sci Rep 5:16358

Li Y-W, Luo X-C, Dan X-M, Huang X-Z, Qiao W, Zhong Z-P, Li A-X (2011) Orange-spotted grouper (*Epinephelus coioides*) TLR2, MyD88 and IL-1β involved in anti-Cryptocaryon irritans response. Fish Shellfish Immunol 30:1230–1240

Li HL, Gu XH, Li BJ, Chen CH, Lin HR, Xia JH (2017) Genome-wide QTL analysis identified significant associations between hypoxia tolerance and mutations in the GPR132 and ABCG4 genes in Nile Tilapia. Mar Biotechnol 19:441–453

Lin G, Wang L, Ngoh ST, Ji L, Orbán L, Yue GH (2018) Mapping QTL for omega-3 content in hybrid saline Tilapia. Mar Biotechnol 20:10–19

Liu F, Sun F, Li J, Xia JH, Lin G, Tu RJ, Yue GH (2013) A microsatellite-based linkage map of salt tolerant tilapia (*Oreochromis mossambicus* x *Oreochromis* spp.) and mapping of sex-determining loci. BMC Genomics 14:1–14

Meyer A, Van De Peer Y (2005) From 2R to 3R: evidence for a fish-specific genome duplication (FSGD). BioEssays 27:937–945

Mori M, Rikitake Y, Mandai K, Takai Y (2014) Roles of nectins and nectin-like molecules in the nervous system. Adv Neurobiol 8:91

Naruse K, Fukamachi S, Mitani H, Kondo M, Matsuoka T, Shu K, Hanamura N, Morita Y, Hasegawa K, Nishigaki R (2000) A detailed linkage map of medaka, Oryzias latipes: comparative genomics and genome evolution. Genetics 154:1773–1784

Nichols KM, Jerri B, Thorgaard GH (2003) Mapping multiple genetic loci associated with Ceratomyxa shasta resistance in Oncorhynchus mykiss. Dis Aquat Org 56:145–154

Ning Y, Liu X, Wang ZY, Guo W, Li Y, Xie F (2007) A genetic map of large yellow croaker Pseudosciaena crocea. Aquaculture 264:16–26

Niu S-F, Jin Y, Xu X, Qiao Y, Wu Y, Mao Y, Su Y-Q, Wang J (2013) Characterization of a novel piscidin-like antimicrobial peptide from Pseudosciaena crocea and its immune response to Cryptocaryon irritans. Fish Shellfish Immunol 35:513–524

Niu D, Du Y, Wang Z, Xie S, Nguyen H, Dong Z, Shen H, Li J (2017) Construction of the first high-density genetic linkage map and

analysis of quantitative trait loci for growth-related traits in Sinonovacula constricta. Mar Biotechnol 19:488–496

Palaiokostas C, Bekaert M, Davie A, Cowan ME, Oral M, Taggart JB, Gharbi K, Mcandrew BJ, Penman DJ, Migaud H (2013) Mapping the sex determination locus in the Atlantic halibut (*Hippoglossus hippoglossus*) using RAD sequencing. BMC Genomics 14:566

Peichel CL, Nereng KS, Ohgi KA, Cole BLE, Colosimo PF, Buerkle CA, Schluter D, Kingsley DM (2001) The genetic architecture of divergence between three spine stickleback species. Nature 414:901–905

Pende D, Bottino C, Castriconi R, Cantoni C, Marcenaro S, Rivera P, Spaggiari GM, Dondero A, Carnemolla B, Reymond N (2005) PVR (CD155) and Nectin-2 (CD112) as ligands of the human DNAM-1 (CD226) activating receptor: involvement in tumor cell lysis. Mol Immunol 42:463–469

Peng W, Xu J, Zhang Y, Feng J, Dong C, Jiang L, Feng J, Chen B, Gong Y, Chen L (2016) An ultra-high density linkage map and QTL mapping for sex and growth-related traits of common carp (*Cyprinus carpio*). Sci Rep 6:26693

Peterson BK, Weber JN, Kay EH, Fisher HS, Hoekstra HE (2012) Double digest RADseq: an inexpensive method for de novo SNP discovery and genotyping in model and non-model species. PLoS One 7: e37135

Rastas P, Paulin L, Hanski I, Lehtonen R, Auvinen P (2013) Lep-MAP: fast and accurate linkage map construction for large SNP datasets. Bioinformatics 29:3128–3134

Sambrook J, Fritsch EF, Maniatis T (eds) (1989) Molecular cloning: a laboratory manual, 2nd edn. Cold Spring Harbor Laboratory Press, New York. (in 3 volumes)

Sawayama E, Tanizawa S, Kitamura S-I, Nakayama K, Ohta K, Ozaki A, Takagi M (2017) Identification of quantitative trait loci for resistance to RSIVD in Red Sea bream (Pagrus major). Mar Biotechnol 19: 601–613

Schoggins JW, Wilson SJ, Panis M, Murphy MY, Jones CT, Bieniasz P, Rice CM (2010) A diverse range of gene products are effectors of the type I interferon antiviral response. Nature 472:481–485

Shao C, Niu Y, Rastas P, Liu Y, Xie Z, Li H, Wang L, Jiang Y, Tai S, Tian Y (2015) Genome-wide SNP identification for the construction of a high-resolution genetic map of Japanese flounder (*Paralichthys olivaceus*): applications to QTL mapping of Vibrio anguillarum disease resistance and comparative genomic analysis. DNA Res 22(2): 161–170

Shih VF-S, Tsui R, Caldwell A, Hoffmann A (2011) A single NFκB system for both canonical and non-canonical signaling. Cell Res 21:86–102

Smith PL, Lombardi G, Foster GR (2005) Type I interferons and the innate immune response—more than just antiviral cytokines. Mol Immunol 42:869–877

Song J, Li Q, Yu Y, Wan S, Han L, Du S (2018) Mapping genetic loci for quantitative traits of golden shell color, mineral element contents, and growth-related traits in Pacific oyster (*Crassostrea gigas*). Mar Biotechnol 20:666–675

Sun B, Greiner-Tollersrud L, Koop BF, Robertsen B (2014) Atlantic salmon possesses two clusters of type I interferon receptor genes on different chromosomes, which allows for a larger repertoire of interferon receptors than in zebrafish and mammals. Dev Comp Immunol 47:275–286

Taharahanaoka S, Miyamoto A, Hara A, Honda S, Shibuya K, Shibuya A (2005) Identification and characterization of murine DNAM-1 (CD226) and its poliovirus receptor family ligands. Biochem Biophys Res Commun 329:996–1000

Taharahanaoka S, Shibuya K, Kai H, Miyamoto A, Morikawa Y, Ohkochi N, Honda S, Shibuya A (2006) Tumor rejection by the poliovirus receptor family ligands of the DNAM-1 (CD226) receptor. Blood 107:1491–1496

Takai Y, Miyoshi J, Ikeda W, Ogita H (2008) Nectins and nectin-like molecules: roles in contact inhibition of cell movement and proliferation. Nat Rev Mol Cell Biol 9:603

Takeda H (2008) Draft genome of the medaka fish: a comprehensive resource for medaka developmental genetics and vertebrate evolutionary biology. Develop Growth Differ 50:S157–S166

Tenoever BR, Ng S-L, Chua MA, Mcwhirter SM, García-Sastre A, Maniatis T (2007) Multiple functions of the IKK-related kinase IKKε in interferon-mediated antiviral immunity. Science 315: 1274–1278

Tsai HY, Hamilton A, Tinch AE, Guy DR, Bron JE, Taggart JB, Gharbi K, Stear M, Matika O, Pong-Wong R (2016) Genomic prediction of host resistance to sea lice in farmed Atlantic salmon populations. Genet Sel Evol 48:47

Van Ooijen JW (2011) Multipoint maximum likelihood mapping in a full-sib family of an outbreeding species. Genet Res 93:343–349

Voorrips RE (2002) MapChart: software for the graphical presentation of linkage maps and QTLs. J Hered 93:77–78

Wang L, Wan ZY, Bai B, Huang SQ, Chua E, Lee M, Pang HY, Wen YF, Liu P, Liu F, Sun F, Lin G, Ye BQ, Yue GH (2015) Construction of a high-density linkage map and fine mapping of QTL for growth in Asian seabass. Sci Rep 5:16358 https://www.nature.com/articles/srep16358#supplementary-information. Accessed 18 Jan 2019

Wang L, Bai B, Huang S, Liu P, Wan ZY, Ye B, Wu J, Yue GH (2017) QTL mapping for resistance to Iridovirus in Asian seabass using genotyping-by-sequencing. Mar Biotechnol 19:517–527

Wu C, Zhang D, Kan M, Lv Z, Zhu A, Su Y, Zhou D, Zhang J, Zhang Z, Xu M (2014) The draft genome of the large yellow croaker reveals well-developed innate immunity. Nat Commun 5:5227

Xiao S, Wang P, Yan Z, Fang L, Yang L, Li JT, Wang ZY (2015) Gene map of large yellow croaker (*Larimichthys crocea*) provides insights into teleost genome evolution and conserved regions associated with growth. Sci Rep 5:18661

Xu J, Zhao Z, Zhang X, Zheng X, Li J, Jiang Y, Kuang Y, Zhang Y, Feng J, Li C, Yu J, Li Q, Zhu Y, Liu Y, Xu P, Sun X (2014a) Development and evaluation of the first high-throughput SNP array for common carp (*Cyprinus carpio*). BMC Genomics 15:307

Xu P, Zhang X, Wang X, Li J, Liu G, Kuang Y, Xu J, Zheng X, Ren L, Wang G, Zhang Y, Huo L, Zhao Z, Cao D, Lu C, Li C, Zhou Y, Liu Z, Fan Z, Shan G, Li X, Wu S, Song L, Hou G, Jiang Y, Jeney Z, Yu D, Wang L, Shao C, Song L, Sun J, Ji P, Wang J, Li Q, Xu L, Sun F, Feng J, Wang C, Wang S, Wang B, Li Y, Zhu Y, Xue W, Zhao L, Wang J, Gu Y, Lv W, Wu K, Xiao J, Wu J, Zhang Z, Yu J, Sun X (2014b) Genome sequence and genetic diversity of the common carp, *Cyprinus carpio*. Nat Genet 46:1212 https://www.nature.com/articles/ng.3098#supplementary-information. Accessed 18 Jan 2019

Ye H, Liu Y, Liu X, Wang X, Wang Z (2014) Genetic mapping and QTL analysis of growth traits in the large yellow croaker *Larimichthys crocea*. Mar Biotechnol 16:729–738

Ying Q, Yong M, Wang J, Chen R, Su YQ, Jia C, Zheng WQ (2016) Analysis of liver and gill miRNAs of *Larimichthys crocea* against Cryptocryon irritans challenge. Fish Shellfish Immunol 59:484–491

Yu Y, Zhang X, Yuan J, Wang Q, Li S, Huang H, Li F, Xiang J (2017) Identification of sex-determining loci in Pacific white shrimp Litopeneaus vannamei using linkage and association analysis. Mar Biotechnol 19:277–286

Yue GH (2014) Recent advances of genome mapping and marker-assisted selection in aquaculture. Fish Fish 15:376–396

Zhang Z, Schwartz S, Wagner L, Miller W (2000) A greedy algorithm for aligning DNA sequences. J Comput Biol 7:203–214

Zhang X, Zhang Y, Zheng X, Kuang Y, Zhao Z, Zhao L, Li C, Jiang L, Cao D, Lu C (2013) A consensus linkage map provides insights on genome character and evolution in common carp (*Cyprinus carpio* L.). Mar Biotechnol 15:275–312

Zhao L, Zhang Y, Ji P, Zhang X, Zhao Z, Hou G, Huo L, Liu G, Li C, Xu P (2013) A dense genetic linkage map for common carp and its integration with a BAC-based physical map. PLoS One 8:e63928

Zhong X, Wang X, Zhou T, Jin Y, Tan S, Jiang C, Geng X, Li N, Shi H, Zeng Q, Yang Y, Yuan Z, Bao L, Liu S, Tian C, Peatman E, Li Q, Liu Z (2017) Genome-wide association study reveals multiple novel QTL associated with low oxygen tolerance in hybrid catfish. Mar Biotechnol 19:379–390

Zhou X, Stephens M (2012) Genome-wide efficient mixed model analysis for association studies. Nat Genet 44:821–824

Zhou H, Chen S, Wang M, Cheng A (2014a) Interferons and their receptors in birds: a comparison of gene structure, phylogenetic analysis, and cross modulation. Int J Mol Sci 15:21045

Zhou Q-J, Su Y-Q, Niu S-F, Liu M, Qiao Y, Wang J (2014b) Discovery and molecular cloning of piscidin-5-like gene from the large yellow croaker (*Larimichthys crocea*). Fish Shellfish Immunol 41:417–420

Zhou T, Liu S, Geng X, Jin Y, Jiang C, Bao L, Yao J, Zhang Y, Zhang J, Sun L (2017) GWAS analysis of QTL for enteric septicemia of catfish and their involved genes suggest evolutionary conservation of a molecular mechanism of disease resistance. Mol Genet Genomics 292:231–242

Zhou Z, Chen L, Dong C, Peng W, Kong S, Sun J, Pu F, Chen B, Feng J, Xu P (2018) Genome-scale association study of abnormal scale pattern in Yellow River carp identified previously known causative gene in European Mirror carp. Mar Biotechnol 20:1–11